Rev. Roum. Sci. Techn.– Électrotechn. et Énerg.
Vol. **70**, *3*, pp. 301–306, Bucarest, 2025

TWO-STAGE INCLINED-PLANE ELECTROSTATIC SEPARATOR FOR MILLIMETER-SIZED PARTICLES

MOKDAD REMADNIA[1], MILOUD KACHI[2]

Keywords: Electrostatic separation; Tribo-electricity; Plastic particles; Recycling; Experimental design methodology.

This paper aims to study and optimize a new configuration of an inclined-plane-type electrostatic separator. The device consists of two inclined planes arranged in a cascade. The design is aimed at efficiently separating millimeter-sized particles, specifically polycarbonate (PC) and polyamide (PA). Preliminary experiments were conducted to investigate the effects of various operating parameters on separation efficiency, including tribo-electric charging time, fluidizing air speed, and the angle between the high-voltage electrodes. The design of experiments (DOE) methodology was employed to model the outcome of the separation process, focusing on two control variables: the length of the electrodes generating the electric field and the applied voltage level. The results revealed the existence of optimal values, resulting in a product recovery rate of 97%, with high purity levels (98% for PC and 96% for PA).

1. **INTRODUCTION**

Materials recycling is one of the cornerstones in the development of a sustainable and ecofriendly industry that meets green economy conditions. In this respect, the quality of the recovered materials is directly linked to the efficiency of the recovery process and its ability to sort mixed materials [1–3]. The electrostatic separation of mixed materials offers efficiency, simplicity, and energy savings in sorting materials based on their electrical properties. Since recovered materials are shredded into small pieces, this particulate nature of the mixture impacts the process as well. It is more convenient to reduce the particle size to smaller dimensions to facilitate their manipulation through electric forces. For all these reasons, the electrostatic separation is applied not only to plastics and metals but also was extended to food separation into components of different properties [4,5]. Depending on the electrical properties of the mixture components, there exist various configurations and separation principals of the electrostatic-based process, which can be categorized into insulator-insulator or insulator-conductor separators. Each of these configurations can use different charging mechanisms, namely tribo-electricity, corona discharge, or even electric induction. Overall, the tribo-electrostatic separation techniques of granular plastic mixtures represent an effective means to recycle several types of plastic or insulating materials [6–8]. The performance of such a process depends on multiple factors, most importantly the charge level acquired by the particles when processed in tribo-electric charging devices before being subjected to the action of electric field forces in electrostatic separators [9]. Unlike corona or inductive charging, which requires an external high-voltage supply, tribo-charging occurs when two surfaces exchange electrical charges upon contact. This phenomenon is commonly attributed to electron, ion, or mass transfer from one body to another [10,11]. By submitting charged particles to a high electric field, the tribo-charged mixtures are typically separated into positively and negatively charged materials, with often a third non-separated quantity failing in the middle [12,13]. The traditional free-fall or roll-type separators suffer from the dominance of the mechanical forces, such as gravity or centrifugal forces, over electrical forces that tend to separate mixture components. Indeed, separation of relatively big particles in the range of a few millimeters in size is a tough task and difficult to control because of the dominance of the particle's weight against the electric force.

In this paper, a novel tribo-electrostatic separator configuration is proposed to sort millimeter-order particles. The separator consists of a double stage of an inclined plane over which divergent electrodes are fixed. The plane inclination is able to reduce the impact of the particle's weight due to the plane support, or reaction force. The suggested separator is an improvement to existing inclined-plane separator initially developed by the authors [14] and can be considered as a complement to the vibrating table case [15]. It increases the recovery rate of plastics without affecting the purity of the recovered products. An optimum design method using the response surface method (RSM) is applied to optimize the operating parameters of the electrostatic process, considering both the recovery and purity of the recovered materials.

2. **EXPERIMENTAL SETUP**

The suggested configuration of the electrostatic separator object of this study can be considered as a series connection between two separators. It consists of two superposed inclined-plane electrostatic separator units, as shown in Fig 1. The positive and negative electrodes are fixed over the plane surfaces in an "inverted V" shape to create a divergent field. The angle between the electrodes middle axis of symmetry and one electrode is noted θ, whereas the inclination angle of the plane relative to horizontal is noted α. Each unit is made of a plastic parallelepiped enclosure that is fixed to an adjustable wooden support. The enclosure's inclination angle (α), adjustable from 0° to 90° from the horizontal, is controlled through a moveable rod fixed between the moveable and static parts of the wooden support. To enable viewing of the separation process, each enclosure has a transparent wall on the front face. The high-voltage electrodes of positive and negative polarity are made of aluminum with an 11 cm height from the plane but with a variable length to assess its effect on the recovery process. The distance between the electrodes increases as the particles travel along the separator. The minimum distance between the electrodes is 8 cm and corresponds to the feeding point of the separator. The angle (θ) formed between the electrodes and their axis of symmetry is adjustable from 3° to 11°. By connecting these electrodes to two tunable high-voltage power supplies with opposing polarity (Models: FuG Elektronik GmbH 83024, Tecknix), a high-intensity electric field is created to attract the charged particles.

[1,2] Electrical Engineering Laboratory – LGEG, University 8 May 1945, B.P.401, Guelma 24000, Algeria
E-mail: remadnia.mokdad@univ-guelma.dz, kachi.m@univ-guelma.dz

DOI: 10.59277/RRST-EE.2025.70.3.3

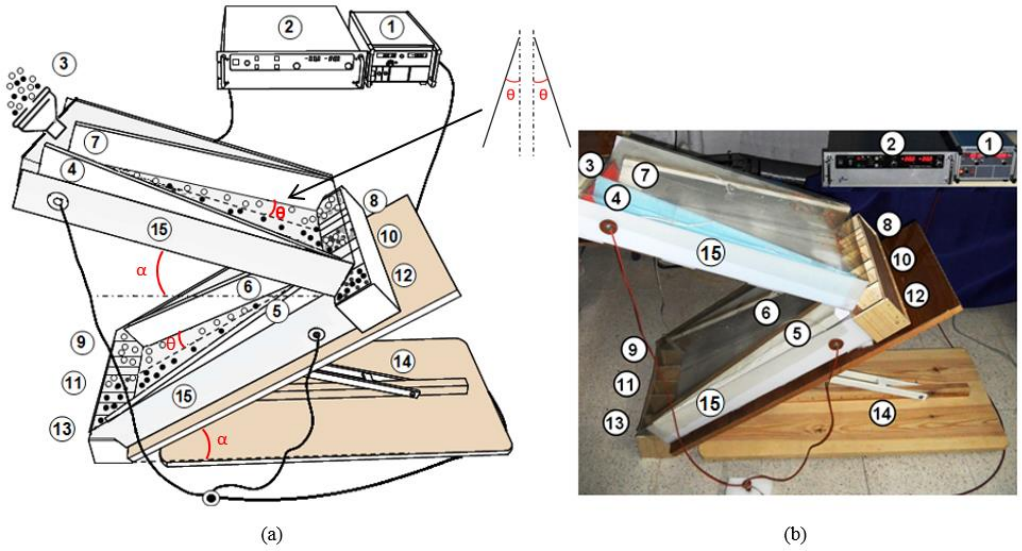

Fig. 1 – Two-stage inclined-plane electrostatic separator for mixed granular plastics: a) schematic representation; b) photography of the electrostatic separator (1 – high-voltage supply-positive polarity, 2 – high-voltage supply-negative polarity, 3 – funnel, 4–5 – plate electrodes connected to the negative polarity; 6–7 – plate electrodes connected to the positive polarity; 8–9 – negatively charged fraction; 10–11 – middlings; 12–13 – positively charged fraction; 14 – movable rods; 15 – insulating enclosure; α – inclination angle of the enclosure; θ – inclination angle of the high-voltage electrodes).

Positively charged particles are drawn to the negative electrode, while negatively charged particles are drawn to the positive electrode. The sorted products in the upper and lower separation sections are recovered in two identical collectors, each box is subdivided into seven compartments: three compartments for the pure product (A), three compartments for the pure product (B), and one compartment for the mixed product. The middling fraction contains a mixture of non-yet separated particles that pass directly to the lower stage to undergo further separation.

3. MATERIALS AND METHOD

The binary mixture used in tribocharging and separation experiments consists of blue polyamide (PA) and orange polycarbonate (PC) particles. Figure 2 shows the size and appearance of the particles. The separation of these polymeric materials poses challenges, as conventional methods (*i.e.*, gravity separation, air separation, and centrifugal separation) are not effective due to their close densities (PA: 1 200 kg/m^3; PC: 1 100 kg/m^3) [6,16]. The experiments were performed with a balanced mixture containing 50 g of PA and 50 g of PC. They were conducted at room temperature in the range of 18 °C to 20 °C, with relative humidity in the range of 39% to 41%.

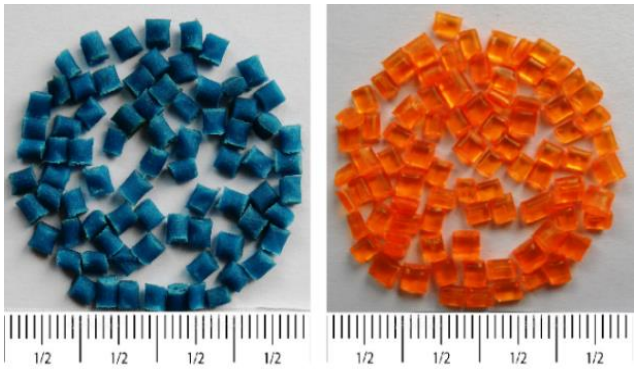

Fig. 2 – Aspect and size of the granular materials; (blue) Polyamide; (orange) Polycarbonate.

The mixed product in the same weight proportions was subjected to the tribocharging process in the fluidization bed device presented in Fig. 3. The charged mixture was then fed into the upper section of the electrostatic separator at a constant feed rate of F = 1.7 g/s through a funnel installed at the inlet of the separator. The inclination angle of the plane (α = 30°) was selected following previous preliminary experiments on single stage [14]. Once the separation is finished, the separated products are removed from the collecting boxes and weighed using a digital balance (precision = 0.01 g). The efficiency of electrostatic separation can be assessed based on the rate of purity and recovery. These indices are defined as follows:

$$\text{Recovery (\%)} = \frac{M_{ci}}{M_{Ti}} \times 100, \tag{1}$$

$$\text{Purity (\%)} = \frac{M_{ci}}{M_{Tc}} \times 100, \tag{2}$$

where M_{ci} – mass of the product i considered collected in the compartment reserved for it; M_{Ti} – total mass of the product i introduced in the separator; M_{TC} – total mass of both products (PA and PC) collected in the same compartment.

The clear difference in color between material particles has made it easier to calculate the recovery and purity of the separated materials. In order to model and optimize the electrostatic process, we used the design of experiments methodology [17,18]. This was done by applying quadratic models associated with a composite factorial experimental design. Using these models, the response (y) will take the following general form:

$$y = a_0 + a_1 x_1 + a_2 x_2 + a_{11} x_1^2 + a_{22} x_2^2 + a_{12} x_1 x_2 \tag{3}$$

where a_i and a_{ij} are the coefficients of the quadratic model, and x_i is the normalized centered value for each factor u_i^*:

$$x_i = (u_i - u_{ic})/\Delta u_i = u_i^* \tag{4}$$

where:

$$u_{ic} = (U_{imax} + U_{imin})/2 \tag{5}$$

$$\Delta u_i = (U_{imax} - U_{imin})/2\,. \quad (6)$$

For the factors that have been considered in this study, namely, the high voltage level U [kV[and the length of the high-voltage electrodes d [cm], the quadratic model of the response y, that is, the recovery and purity rates of each collected product, will take the following form:

$$y = a_0 + a_1 U^* + a_2 d^* + a_{11} U^{*2} + a_{22} d^{*2} + a_{12} U^* d^*\,. \quad (7)$$

The obtained results were analyzed with MODDE 8.0 software [19], which computes the coefficients of the mathematical models, creates the response contours, and identifies the best adjustments of the experimental parameters for optimizing the electrostatic process.

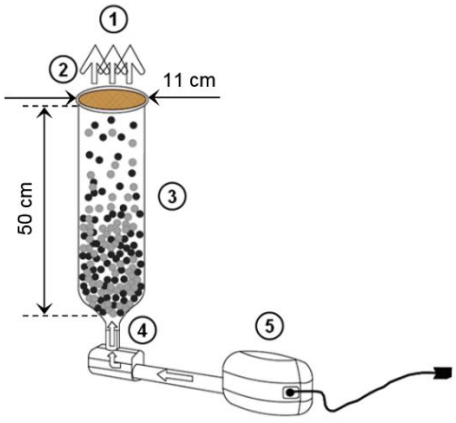

Fig. 3 – Schematic representation of the fluidized bed device: 1 – air output; 2 – filter; 3 – tribocharging chamber made of polyethylene terephthalate (PET); 4 – air admission; 5 – air blower.

4. RESULTS AND DISCUSSION

4.1. EFFECT OF THE CHARGING TIME ON THE ACQUIRED CHARGE

The charging time Tch of PA and PC particles inside the fluidized-bed device was increased up to 4 minutes for a constant fluidizing air speed (S = 15 m/s). After tribocharging, the electric charge of each material was measured by pouring the material into a Faraday pail connected to an electrometer (Keithley Instruments, model 6514). Then they were weighed using an electronic balance. The obtained charge-to-mass ratios are shown in Fig. 4 as a function of the tribocharging time.

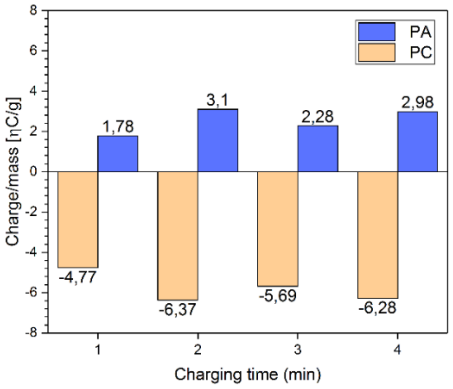

Fig. 4 – Evolution of the charge per mass ratio of PA and PC particles as a function of charging time (Air speed: S = 15 m/s).

The best-acquired charge by the particles is achieved when the time spent in the fluidized bed reaches T_{ch} = 2 minutes. In fact, in the case of 2 minutes of tribocharging, the values of the acquired charge measured for the two products PC and PA are (–6.37 ηC/g) and (+3.1 ηC/g), respectively. After two minutes in the tribocharging device, the charging efficiency of both materials does not rise; rather, it starts to saturate. Therefore, at the appropriate charging time, the particles can acquire an optimal electric charge equal to their saturation value.

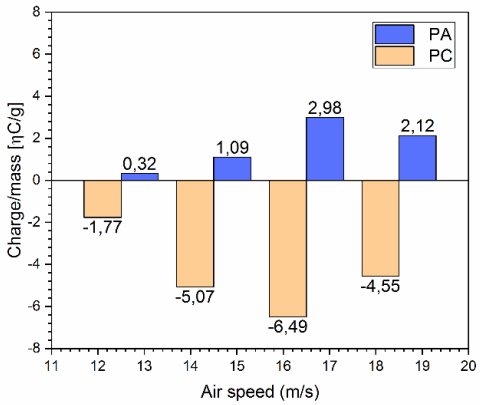

Fig. 5 – Evolution of the charge per mass ratio of PA and PC particles as a function of the fluidizing air speed (Charging time: T_{ch} = 2 min).

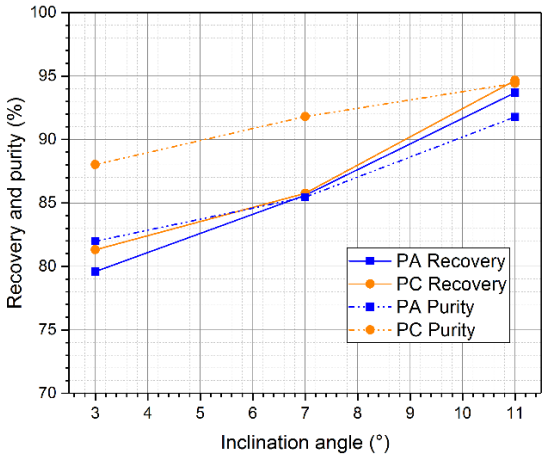

Fig. 6 – Evolution of the recovery and purity rates of PA and PC in the corresponding boxes as a function of the inclination angle between electrodes (charging time: T_{ch} = 2 min, air speed: S = 16.5 m/s, applied voltage: U = 8 kV).

4.2. IMPACT OF FLUIDIZING AIR SPEED ON THE PARTICLE'S CHARGE

Figure 5 shows the influence of the air flow rate in the fluidized bed. As it can be seen, in this case, this parameter also has a significant impact on the acquired charge. For both products, the measured value of the acquired charge increases with fluidizing air speed, then saturates for values higher than 16.5 m/s. The higher air speed is accompanied by more numerous and stronger collisions between the particles and the walls of the fluidization bed device. Therefore, the charge-to-mass ratio can be improved by adjusting the air flow rate in the fluidized bed tribocharging device. Thus, in the case of our tribocharging device, the value of 16.5 m/s of air speed was determined to be optimal for achieving a high charge-to-mass ratio.

4.3. INFLUENCE OF THE ELECTRODE DIVERGENCE ANGLE ON SEPARATION EFFICIENCY

To investigate the effect of the divergence angle (θ) of the high-voltage electrodes on the separation efficiency, three different angles are considered (*i.e.*, θ = 3°, 7°, and 11°) for the electrodes mounted in each stage of the separator. The mechanical design of the separator imposes a maximum value of θ = 11° and a lower value of θ = 3°. Figure 6 depicts the evolution of the recovery and purity rates of both PC and PA particles as a function of the inclination angle. Raising the inclination angle from 3 to 11° causes a significant increase in separation efficiency. The best results in recovery and purity are obtained when the angle between HV electrodes is in its maximum value θ = 11°.

4.4. MODELING OF THE ELECTRO-SEPARATION PROCESS

In this section, the experimental modeling of the electrostatic process was studied with the most influential factors. The other operating conditions were kept constant at the following values:

- Charging time: T_{ch} = 2 min.
- Fluidization air speed: S = 16.5 m/s.
- Divergence angle of the electrodes: θ = 11°.

Based on the results of several preliminary separation tests, the limit values of the two control variables of the process were established as follows:

- Applied voltage (U): U_{min} = 6 kV and U_{max} = 10 kV.
- Length of high-voltage electrodes (d): d_{min} = 75 cm and d_{max} = 150 cm.

The output variables of the system are the recovery and the purity rate of PC and PA particles. Figure 7 shows the experiments of a face-centered central composite design, allowing the use of Response Surfaes Modeling. It consists of four experiments located at the square's corners (round points *A*, *B*, *C*, and *D*), four experiments located at the center of each side of factorial space (stars points *E*, *F*, *G*, and *H*), and three replicated experiments done at the central point (square point *M*).

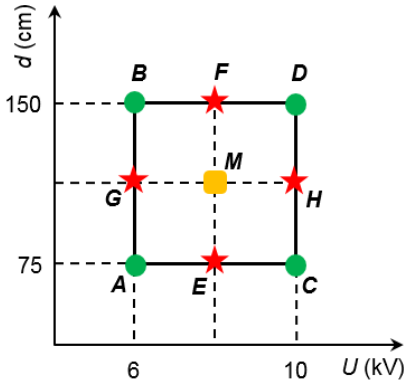

Fig. 7 – Diagram of experiments with a face-centered central composite design with two factors: applied voltage U (U_{min} = 6 kV and U_{max} = 10 kV) and length of high-voltage electrodes d (d_{min} = 75 cm and d_{max} = 150 cm).

The results of the 11 experiments are reported in Table 1. The following mathematical models are obtained for the collected materials:

$$R(PC) = 95.46 + 10.74U^* - 20.32d^* - 26.79U^{*2} - 17.39d^{*2} - 8.96U^*d^* \quad (8)$$

$$R(PA) = 96.07 + 4.66U^* - 7.24d^* - 21.78U^{*2} - 10.34d^{*2} + 5.61U^*d^* \quad (9)$$

$$P(PC) = 94.49 + 13.71U^* - 16.34d^* - 25.81U^{*2} - 16.64d^{*2} - 10.87U^*d^* \quad (10)$$

$$P(PA) = 94.27 + 17.05U^* - 8.93d^* - 25.70U^{*2} - 8.23d^{*2} - 2.93U^*d^* . \quad (11)$$

Table 1

Results of the face-centered central composite design for the study of the electrostatic separation process

Exp.No.	Factors		Responses			
	U (kV)	d (cm)	$R(PC)$ (%)	$R(PA)$ (%)	$P(PC)$ (%)	$P(PA)$ (%)
1	6	75	52.32	71.89	44.81	50.5
2	10	75	92.19	69.67	93.11	90.31
3	6	150	29.48	47.16	33.74	38.08
4	10	150	33.5	67.41	38.55	66.16
5	6	112.5	57.17	69.13	53.06	49.5
6	10	112.5	77.73	79.08	82.23	83.93
7	8	75	97.06	93.77	93.04	92.71
8	8	150	56.64	77.31	60.58	75.67
9	8	112.5	96.39	96.19	94.27	95.04
10	8	112.5	95.14	95.88	96.31	94.83
11	8	112.5	97.29	96.52	94.98	96.66

Table 2

Values of the statistical indexes R2 and Q2 of the responses

Indexes	$R(PC)$ (%)	$R(PA)$ (%)	$P(PC)$ (%)	$P(PA)$ (%)
R2	0.996	0.997	0.996	0.989
Q2	0.989	0.986	0.988	0.966

MODDE 8.0 was used to assess the goodness of fit (R2) and the goodness of prediction (Q2). Based on the values of R2 and Q2 presented in Table 2, the two statistical coefficients were close to 1 for the four quadratic polynomials (8), (9), (10) and (11), which means that they were quite satisfactory. The coefficients values linked to the factors in the models measure the degree of influence of each factor and the interaction between them.

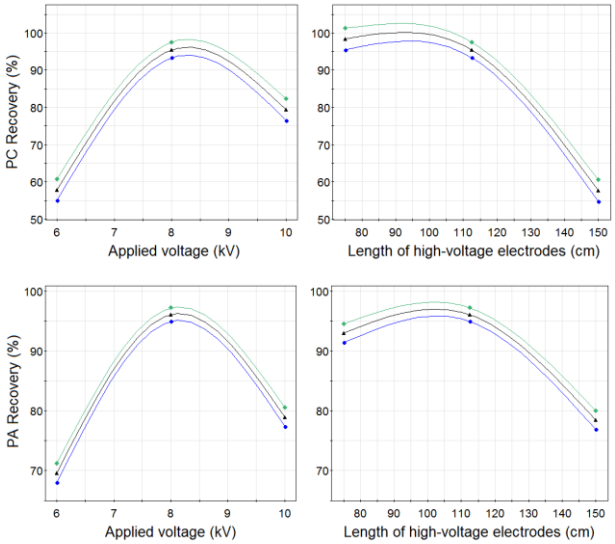

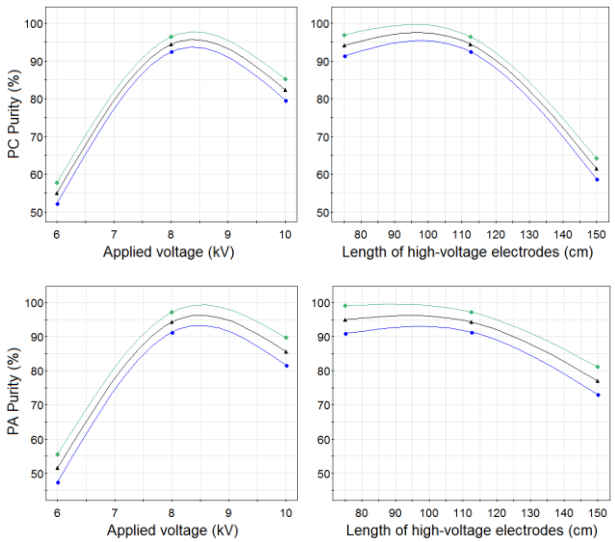

Fig. 8 – Recovery and purity rates predicted by MODDE 8.0 as a function of the applied voltage U (kV) and the length of the high-voltage electrodes d (cm). In each case, the other variable is kept constant and set to its central value (U = 8 kV and d = 112.5 cm). The upper and lower curves define the 95 % confidence interval.

Figure 8 illustrates the influence of each factor on the four responses. Within the domain of the two factors, the contour plots shown in Fig. 9 and Fig.10 demonstrate the effect of the interaction between the variables on the responses $R(PC)$, $R(PA)$, $P(PC)$, and $P(PA)$, respectively. We created contour plots to gain a deeper comprehension of the interaction between the two control variables. We used the Student's test to evaluate the statistical significance of each mathematical model's coefficients. The results indicate that all the effects (*i.e.*, the coefficients of U^* and d^*) and the interaction between them (*i.e.*, the coefficient of U^*d^*) are significant.

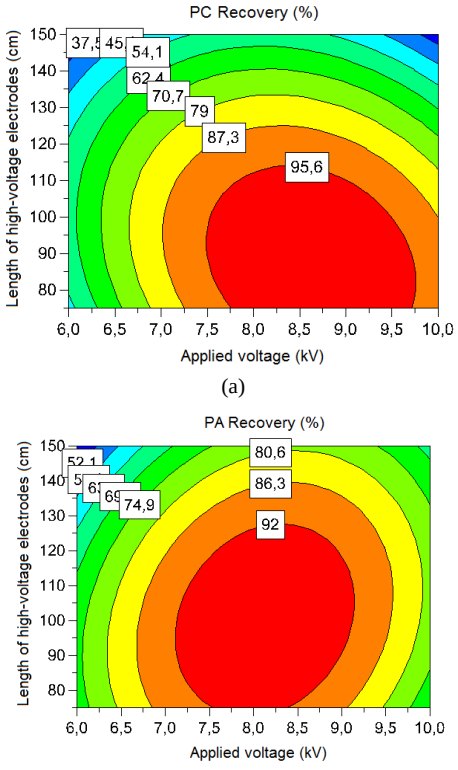

Fig. 9 – MODDE-computed equal-response contours: a) PC recovery; b) PA recovery.

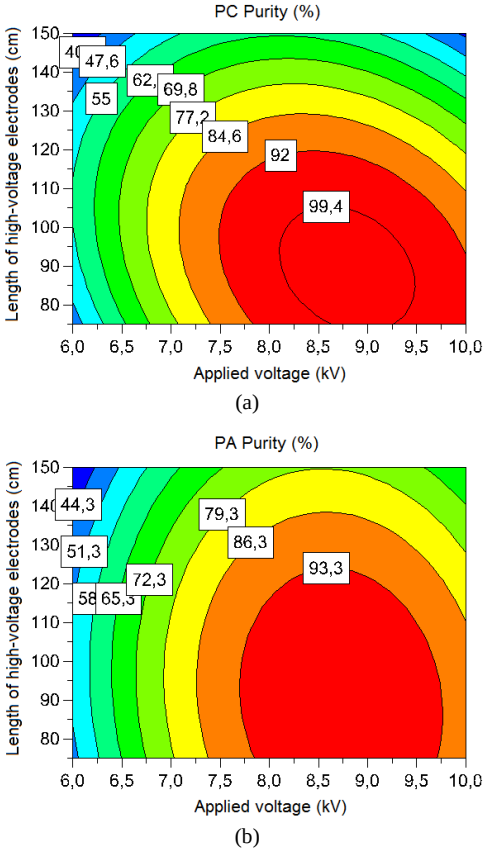

Fig. 10 – MODDE-computed equal-response contours: a) PC purity; b) PA purity.

Based on these results, the increase in the applied voltage from 6 kV to 8.5 kV significantly improves the recovery rate and purity of both products. The electric field forces acting on the particles are stronger at higher voltages, which enhances the effectiveness of electrostatic separation. However, further increase in the applied voltage beyond 8.5 kV decreases the separation efficiency, as can be easily observed in Fig. 8. The length of the electrodes seems to have the same effect as the applied voltage; the increase in the length of the electrodes from 75 cm up to 100 cm improves the separation efficiency. However, the separation efficiency decreases significantly when the length exceeds 100 cm. This can be explained by the fact that at higher electrode lengths, the particles perform a bouncing motion between the two high-voltage electrodes, which affects their fall trajectories towards the collector boxes. Therefore, better electrostatic separation results can be obtained by appropriately correlating the applied voltage value and the length of the high-voltage electrodes.

4.5. OPTIMAL OPERATION CONDITIONS

The optimization step of this electrostatic process should enable the identification of factor values that lead to the highest recovery and purity rates of the recovered products. The Optimizer subroutine of MODDE 8.0 allows the possibility of identifying the optimal operation conditions of the process. The mathematical models obtained indicate that we should obtain the operation set point, or the highest recovery and purity rate of PC and PA materials, for an applied voltage of U = 8.29 kV and a length of high-voltage electrodes of d = 103.66 cm, for which the predicted recovery rates of PC and PA were 100 % and 97.22%, respectively, and the predicted purity rates of PC and PA

were 99.28% and 97.99%, respectively. A verification experiment conducted by applying the obtained optimal values leads to the following results: $R(PC) = 98.10\%$, $R(PA) = 97.71\%$, $P(PC) = 98.04\%$, and $P(PA) = 96.89\%$. The results from the experiment and predicted models were in very good agreement. In a previous paper [14], the classic configuration of the inclined-plane electrostatic separator achieves a relatively low recovery rate of 70% with product purity of roughly 97% for PA and 98% for PC. However, with the configuration proposed in this paper, it is possible to achieve a significantly higher recovery rate, along with very high purity levels.

5. **CONCLUSIONS**

The paper presents experimental results of a double-stage inclined plane electrostatic separation. The developed separator is suitable for sorting large particles in the range of a few millimeters in size. The results of the laboratory-scale experiments pointed out the following conclusions:

- The efficiency of the tribo-electric charging process depends on the fluidizing air speed and the charging time.
- Increasing the inclination angle between the high-voltage electrodes has a positive impact on the separation efficiency. An inclination angle of 11° yields the best results.
- The experimental design methodology showed the existence of optimum values of the electrode length and applied voltage amplitude. A correlation between these parameters is essential for process optimization.

CREDIT AUTHORSHIP CONTRIBUTION STATEMENT

Remadnia Mokdad – Conceptualization, formal analysis, investigation, methodology, software, writing-review, and editing. Kachi Miloud – Methodology, supervision, validation, writing review, and editing.

Received on 22 September 2024

REFERENCES

1. M. Burgess, H. Holmes, M. Sharmina, M. P. Shaver, *The future of UK plastics recycling: One bin to rule them all*, Resources, Conservation and Recycling, **164**, pp. 105191 (2021).
2. N. Kadri, W. Krika, A. N. Ayad, T. Rouibah, F. B. Ahmet, E. Kadir, I. R. Bara, S. S. M. Ghoneim, *Recovery of non-ferrous particles from recycling neon lamps by magnetic induction separator*, Rev. Roum. Sci. Techn. – Électrotechn. Et Énerg., **69**, *3*, pp. 283–286 (2024).
3. L. M. Dumitran, L.V. Badicu, M.C. Plopeanu, L. Dascalescu, *Efficiency of dual wire-cylinder electrodes used in electrostatic separators*, Rev. Roum. Sci. Techn. – Électrotechn. et Énerg., **55**, *2*, pp. 171–180 (2010).
4. M. Kahaleras, M. Remadnia, M. Kachi, A. Nadjem, *Semolina extraction from wheat bran using an electro-separation process*, Journal of Food Processing and Preservation, **45**, *4*, e15352 (2021).
5. S. Tabtabaei, D. Konakbayeva, A.R. Rajabzadeh, R.L. Legge, *Functional properties of navy bean (Phaseolus vulgaris) protein concentrates obtained by pneumatic tribo-electrostatic separation*, Food Chemistry, **283**, pp. 101–110 (2019).
6. T. Phengsaart, P. Julapong, C. Manositchaikul, P. Srichonphaisarn, M. Rawangphai, O. Juntarasakul, K. Aikawa, S. Jeon, I. Park, C.B. Tabelin, M. Ito, *Recent Studies and Technologies in the Separation of Polyvinyl Chloride for Resources Recycling: A Systematic Review*, Sustainability, **15**, *18*, pp. 13842 (2023).
7. A. Iuga, A. Samuila, R. Morar, M. Bilici, L. Dascalescu, *Tribocharging techniques for the electrostatic separation of granular plastics from waste electric and electronic equipment*, Particulate Science and Technology, **34**, *1*, pp. 45–54 (2016).
8. J. Li, Z. Xu, *Compound tribo–electrostatic separation for recycling mixed plastic waste*, Journal of Hazardous Materials, **367**, pp. 43–49 (2019).
9. S. Mouhoub, M. Kachi, N. Zouzou, *Influence of the initial charge on the triboelectrification of millimeter size set of particles in an inclined tube*, Powder Technology, **428**, pp. 118862 (2023).
10. Y. Shen, D. Tao, L. Zhang, H. Shao, X. Bai, X. Yu, *An experimental study of triboelectrostatic particle charging behavior and its associated fundamentals*, Powder Technology, **429**, pp. 118880 (2023).
11. S. Matsusaka, H. Maruyama, T. Matsuyama, M. Ghadiri, *Triboelectric charging of powders: A review*, Chemical Engineering Science, **65**, *22*, pp. 5781–5807 (2010).
12. M. Maammar, T. Zeghloul, W. Aksa, S. Touhami, I. Achouri, L. Dascalescu, *Factors that influence the trajectories of charged insulating particles in roll–type electrostatic separators*, Journal of Electrostatics, **115**, pp. 103672 (2022).
13. P. M. Ireland, *Modelling dense particle streams during free–fall electrostatic separation*, Powder Technology, **434**, pp. 119290 (2024).
14. A. Nadjem, M. Kachi, K. Rouagdia, M. Remadnia, *Experimental Study of an Inclined-Plane Electrostatic Separator*, Proceedings of the Third International Symposium on Materials and Sustainable Development, Cham: Springer International Publishing, pp. 439–450 (2018).
15. I. E. Achouri, G. Richard, T. Zeghloul, K. Medles, L. Dascalescu, *New Vibrating–Table–Type Tribo–Electrostatic Separator for Selective Sorting of Granular Plastic Wastes*, IEEE Transactions on Industry Applications, **60**, *2*, pp. 3537–3542 (2024).
16. S. M. Al-Salem, P. Lettieri, J. Baeyens, *Recycling and recovery routes of plastic solid waste (PSW): A review*, Waste Management, **29**, *10*, pp. 2625–2643 (2009).
17. K. Rouagdia, L. Dascalescu, *Robust optimum operating conditions for AC corona neutralization of insulating materials*, Rev. Roum. Sci. Techn. – Électrotechn. et Énerg., **65**, *1–2*, pp. 5–10 (2020).
18. S. V. Silva, J.S. Cardoso, V. Silva, J.S. Cardoso, *Response Surface Methods – Theory, Applications and Optimization Techniques*, IntechOpen, London, UK. (2024).
19. ***User Guide and Tutorial to MODDE: Version 8.0, Umetrics, Umea, Sweden (2006).